Eur. Phys. J. B **24**, 511–524 (2001)

THE EUROPEAN PHYSICAL JOURNAL B

EDP Sciences
© Società Italiana di Fisica
Springer-Verlag 2001

Thermodynamics and transport in an active Morse ring chain

J. Dunkel[a], W. Ebeling, and U. Erdmann

Institute of Physics, Humboldt University Invalidenstrasse 110, 10115 Berlin, Germany

Received 21 July 2001

Abstract. We investigate the stochastic dynamics of an one-dimensional ring with N self-driven Brownian particles. In this model neighboring particles interact *via* conservative Morse potentials. The influence of the surrounding heat bath is modeled by Langevin-forces (white noise) and a constant viscous friction coefficient γ_0. The Brownian particles are provided with internal energy depots which may lead to active motions of the particles. The depots are realized by an additional nonlinearly velocity-dependent friction coefficient $\gamma_1(v)$ in the equations of motions. In the first part of the paper we study the partition functions of time averages and thermodynamical quantities (*e.g.* pressure) characterizing the stationary physical system. Numerically calculated non-equilibrium phase diagrams are represented. The last part is dedicated to transport phenomena by including a homogeneous external force field that breaks the symmetry of the model. Here we find enhanced mobility of the particles at low temperatures.

PACS. 05.45.-a Nonlinear dynamics and nonlinear dynamical systems – 05.70.Ln Non-equilibrium and irreversible thermodynamics – 05.40.-a Fluctuation phenomena, random processes, noise and Brownian motion

1 Introduction

The theory of passive Brownian motion [1] describes the dynamics of a macroscopic particle in a surrounding heat bath (*e.g.* liquid). It links viscous friction with the fluctuations reflecting the underlying microscopic (*e.g.* atomic, molecular) structure of the bath. Several models of self-driven Brownian particles were developed within the theory of active Brownian motion and also recently used for modeling some new types of complex motion [2–5]. Here we will continue the discussion of an one-dimensional model of active Brownian particles with conservative nonlinear Morse interactions between next neighbors. In [6] we introduced this system and concentrated basically on the effects of the nonlinear deterministic dynamics corresponding to the temperature limit $T \to 0$ when there are no fluctuations in the bath. We studied several types of attractors representing different types of active stationary motions (*e.g.* stable nonlinear waves or cluster rotations) and also began the discussion of the model at non-zero temperature which we would like to extend here.

The Morse potential (Fig. 1) for the interaction between two particles reads

$$U_i^M = \frac{a}{2b}\left(\mathrm{e}^{-br_i} - 1\right)^2 - \frac{a}{2b} \tag{1}$$

and it is closely related to the well-known Toda potential [7]

$$U_i^T = \frac{a}{b}\left(\mathrm{e}^{-br_i} - 1\right) + ar_i. \tag{2}$$

[a] e-mail: dunkel@physik.hu-berlin.de

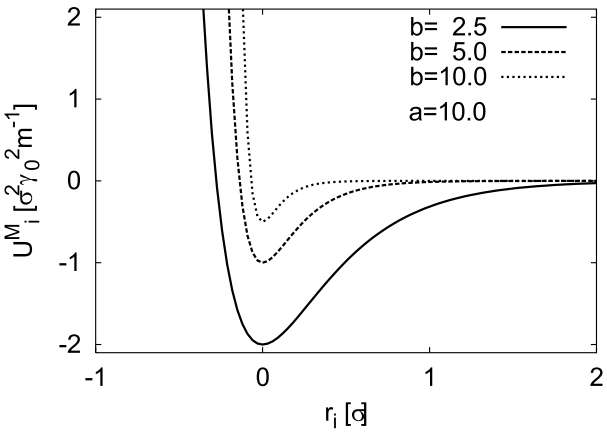

Fig. 1. Morse potential U_i^M plotted for $a = 1$ ($[a] = \sigma\gamma_0^2 m^{-1}$ and $[b] = \sigma^{-1}$).

In (1) and (2) the parameter a controls the amplitude of the corresponding force while the parameter b is responsible for the stiffness of the spring connecting two interacting particles. The relative coordinates

$$r_i = x_{+1} - x_i - \sigma \tag{3}$$

represent the distance between two neighboring particles at positions x_i and x_{i+1} reduced by the equilibrium length σ of the springs. In this notation Morse and Toda potential have their minimum at $r_i = 0$ *i.e.* both potentials

are repulsive for $r_i < 0$ and attracting for $r_i > 0$. The main difference between the two types of interactions is the behavior for $r_i \to \infty$. In contrast to the Toda force the Morse force tends to zero for long distances between the particles. This difference leads to new physical effects in a Morse chain (*e.g.* formation of clusters) if the particle density

$$n = N/L \tag{4}$$

is sufficiently low [6]. In (4) N denotes the number of Brownian particles on the ring and L the length of the ring.

One reason for the special interest in $1d$-Toda models is the existence of exact solutions for the conservative lattice and also for the statistical equilibrium thermodynamics [7,8]. The advantage of the Morse potential compared with the Toda potential is that it represents a more realistic interaction, *e.g.* it is similar to the well-known Lennard-Jones potential describing molecular interactions. Unfortunately, there are neither many analytical results nor exact solutions for the dynamics of a Morse lattice [6,9].

A first approach to investigate active Toda rings with the aim to model dissipative solitons was given recently in [5,10,11]. In these papers it was shown theoretically, numerically and experimentally that in active Toda rings stable running soliton excitations may be generated. The active Brownian particles in our model are characterized by the ability to take up energy from an external reservoir, to store this energy in internal depots and to convert depot energy into kinetic energy of motion. The energy exchange process between the particles and the external reservoir is supposed to be deterministic and independent of the fluctuations in the heat bath. This depot model was proposed in [4,12,13] and gives a nonlinearly velocity dependent contribution $\gamma_1(v)$ to the effective friction coefficient $\gamma(v)$ of a Brownian particle

$$\gamma(v) = \gamma_0 + \gamma_1(v). \tag{5}$$

In (5) the parameter γ_0 is the constant coefficient of viscous friction from the interaction between particle and heat bath. Hence, *via* $\gamma_1(v) = 0$ our model may be reduced to the corresponding thermodynamical equilibrium system.

With respect to previous investigations [6] all results found for active Toda chains [5,10,11] remain valid for an active Morse ring with high particle density $n \gg \sigma^{-1}$ since in this limit a Morse ring with stiffness parameter b converges to a Toda ring with stiffness parameter $2b$. Only for low particle densities the active Morse ring shows new effects (*e.g.* formation of rotating clusters) that can not be observed in Toda chains. Concisely, the active Morse ring we intend to deal with may be driven from an exact soluble equilibrium Toda system [7,8] to states featuring active motions and clustering phenomena.

The paper is organized as follows. In Section 2 we introduce the equations of motion and discuss the dynamics and statistics of non-interacting active Brownian particles. Section 3 is dedicated to studies of active Morse rings at non-zero temperature of the heat bath. We investigate the system with regard to coherent motions as well as from the thermodynamical point of view (*e.g.* non-equilibrium phase diagrams). In Section 4 we study transport in presence of a homogeneous external field.

2 Stochastic dynamics of active Brownian particles

2.1 Equations of motion

Our one-dimensional model of active Brownian particles consists of N point masses m located at the coordinates x_i $(i = 1, \ldots, N)$. The particles are connected to their next neighbors at both sides by pair interactions

$$F_i = F(x_{i-1}, x_i, x_{i+1}). \tag{6}$$

The conservative force on the ith particle with coordinate x_i may be obtained by differentiating the full potential energy of the ring

$$U = \sum_{i=1}^{N} U_i^M \tag{7}$$

with respect to x_i. In order to realize a ring of length L we choose the periodic boundary conditions

$$x_{i+N} = x_i + L. \tag{8}$$

If we imagine the particles to be surrounded by a heat bath of smaller particles the Langevin equations for the individual velocities $v_i = \mathrm{d}x_i/\mathrm{d}t$ are given by

$$m\frac{\mathrm{d}}{\mathrm{d}t}v_i - F_i = -\gamma_0 v_i + A_i(t). \tag{9}$$

The (dissipative) terms on the r.h.s. represent the interaction between a Brownian particle and the heat bath. In this notation the viscous friction coefficient γ_0 is defined by

$$\gamma_0 = \frac{m}{\tau_{\mathrm{rel}}} \tag{10}$$

where τ_{rel} is the mean relaxation time of the Brownian particles due to viscous friction in the heat bath. The stochastic Langevin forces A_i are determined by

$$\langle A_i(t)\rangle = 0 \qquad \langle A_i(t')A_j(t)\rangle = 2D\delta_{ij}\delta(t'-t), \tag{11}$$

i.e. they represent Gaussian white noise reflecting the atomic or molecular structure of the bath. For (9) the temperature T of the heat bath, D and γ_0 are connected *via* the Einstein relation

$$D = \gamma_0 T. \tag{12}$$

In (12) we used an unit temperature $[T] = k_{\mathrm{B}}^{-1}$ with k_{B} denoting the Boltzmann constant. The situation described so far corresponds to a typical equilibrium system characterized by purely passive friction and it obeys the standard equilibrium statistics.

2.2 Depot model for self-driven particles

As indicated before we would like to investigate the effects of active friction corresponding to an additional nonlinearly velocity dependent friction term in the equations of motions (9). As a simple model of active friction we consider the friction force proposed in [4,12,13]

$$\gamma_1(v)\, v = -\frac{q}{(c/d_2) + v^2} v \tag{13}$$

that models active particles carrying refillable energy depots. In (13) the positive quantity q describes the flux of energy from an external reservoir or field into the depots carried by the particles. The parameter $c > 0$ is connected to internal dissipation and $d_2 > 0$ controls the conversion of the energy taken up from the external field into kinetic energy. In fact, the parameter q and the ratio

$$\kappa = c/d_2 \tag{14}$$

are the essential parameters of this model. Thus the parameter situation $\kappa = 0$ describes particles without internal dissipation. Using the effective friction coefficient $\gamma(v_i)$ defined in (5) we may write down the full Langevin equation for our model

$$m\frac{\mathrm{d}}{\mathrm{d}t}v_i - F_i = -\gamma(v_i)v_i + A_i(t). \tag{15}$$

In case of $q = 0$ (no feeding with external energy) or $\kappa = \infty$ (no energy conversion) there is no pumping (*i.e.* $\gamma_1(v_i) = 0$) and (15) coincides with the Langevin equations (9) corresponding to the equilibrium system. For convenience we introduce a new parameter

$$\mu = \frac{q}{\gamma_0} - \kappa \tag{16}$$

and rewrite

$$\gamma(v) = \gamma_0\left(1 - \frac{\kappa + \mu}{\kappa + v^2}\right) = \gamma_0\, \frac{v^2 - \mu}{\kappa + v^2}. \tag{17}$$

Obviously the parameter μ plays the role of a bifurcation parameter since $\gamma(v) = 0$ if $v = \pm\sqrt{\mu}$. The effect of the effective friction force $-\gamma(v)v$ on the dynamics can also be illustrated by introducing the effective dissipative potential

$$\begin{aligned} V_{\mathrm{diss}}(v) &= \int \gamma(v)\, v\, \mathrm{d}v \\ &= \frac{1}{2}\,\gamma_0\,[v^2 - (\kappa + \mu)\,\ln(\kappa + v^2)]. \end{aligned} \tag{18}$$

The shape of V_{diss} for different values of μ and κ can be seen in Figure 2.

For $\mu > 0$ the dissipative potential is bistable *i.e.* it has two minima at $\pm\sqrt{\mu}$. This means that a free pumped Brownian particle aims to reach one of these velocities in the stationary state corresponding to so-called active or self-driven motion. On the other hand, parameter values

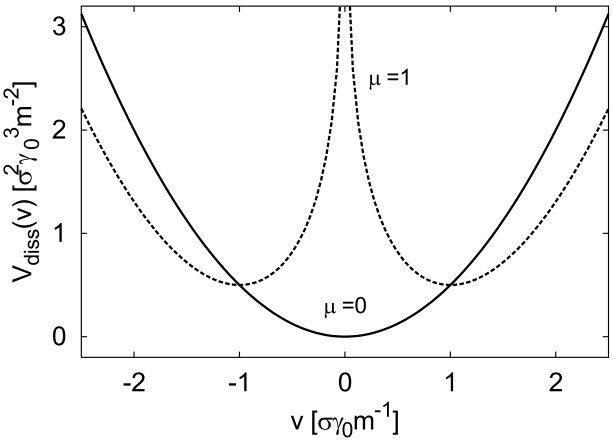

(a) $\kappa = 0$.

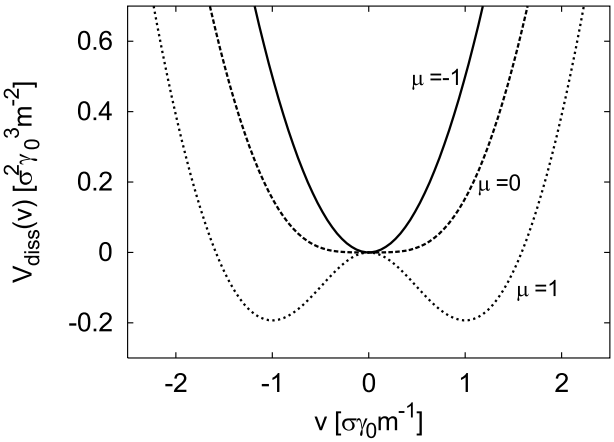

(b) $\kappa = 1$.

Fig. 2. Dissipative potential $V_{\mathrm{diss}}(v)$ (units are $[\kappa] = [\mu] = \sigma^2\gamma_0^2 m^{-2}$). For (a) $\kappa = 0$ and $\mu > 0$ the dissipative potential is bistable and diverges for $v \to 0$. In case of $\mu \leq 0$ it is monostable.

$\mu < 0$ lead to a damped system. Then the only stable, stationary velocity is $v = 0$, *i.e.* all motions come to rest after a certain relaxation time. According to (17) for $\mu > 0$ the effective friction coefficient $\gamma(v)$ converges to γ_0 for large velocities $v^2 \gg \mu$, but for small velocities $v^2 < \mu$ the $\gamma(v)$ is negative. This region corresponds to pumping with free energy on the cost of the depots and the dynamics develops active forms of motions. For simplicity we will assume throughout this paper that the external energy reservoir providing the energy for the depots is not explicitly time dependent. The generalization to active friction on the basis of finite time-dependent depots which can be filled again at discrete places (filling stations) is straightforward according to our earlier work [4,12,13].

Before we begin the analysis of the model it may be useful to give one motivating interpretation for the model. In some very simple sense one can think of the Brownian particles to represent small biological objects (*e.g.* bacteria in a liquid) which are able to move actively if there is

enough food (the energy reservoir). At intermediate distances they feel attracted by each other but due to their spatial extension (which is characterized by σ) there is also a repulsive component for very short distances. The stochastic force models a liquid that can take different temperature values and contains the organisms.

Characteristic units

In order to reduce the number of parameters in our model it is useful to choose characteristic units of reference. As we intend to investigate homogeneous rings we may use a unit system where $m = 1$, $\sigma = 1$ and $\gamma_0 = 1$. The first two choices simply correspond to fixing unit mass and unit distance. The first and third together give a characteristic unit time because of (10). Thus the unit time in our model is given by the relaxation time due to viscous friction in absence of pumping. Choosing this system of reference automatically implies that all remaining parameters are measured in this unit system. With these considerations our working equation is given by

$$\frac{\mathrm{d}}{\mathrm{d}t}v_i - F_i = \left[\frac{\kappa+\mu}{\kappa+v_i^2} - 1\right]v_i + A_i(t) \tag{19}$$

where now $\mu = q - \kappa$.

2.3 Fluctuation-dissipation-theorem

At this point it is worth to have a look at the fluctuation-dissipation-theorem (FDT) given by the Einstein relation (12). The FDT links the amplitude D of the stochastic force with the physical temperature T of the heat bath and the viscous friction coefficient γ_0. For passive Brownian motion this result is obtained by the condition of statistical equilibrium between Brownian particles and surrounding medium. An important question to answer is: Does this FDT still make sense in our model?

As explained in the introduction, we assume that in our model the energy transfer from the external reservoir and the conversion of depot energy into kinetic energy of the particles are completely independent of the fluctuations in the heat bath, *i.e.* it is a property of the particles exclusively. In addition, we want this model to represent a classical equilibrium system in absence of the deterministic pumping and at high velocities (limit of viscous friction), hence we expect a Maxwell-like velocity distribution for these two limits only. From this point of view it is sensible to postulate that the Einstein relation (12) is the valid FDT also for the non-equilibrium system. In other words, we suppose that the noise generated by the heat bath is not influenced by the deterministic pumping which is supposed to be a property of the Brownian particles themselves. In the characteristic units of the model we even have

$$D = T.$$

This approach means, that we neglect feedback between particles and heat bath, which is likely to occur in real systems.

An extensive discussion of non-equilibrium models where the fluctuation dissipation theorem differs from the Einstein relation (12) *e.g.* models with velocity dependent viscous friction coefficients may be found in [14].

2.4 Statistics of free particles

Before we go on to discuss the Morse rings let us briefly look at the stationary probability density $f(v)$ of free active Brownian particles. This situation corresponds to choosing $a = 0$. With respect to the considerations in Section 2.3 the density function of a single free particle is determined by the following Fokker-Planck-Equation (FPE) [13,14]

$$\frac{\partial f}{\partial t} = T\frac{\partial^2 f}{\partial v^2} + \frac{\partial}{\partial v}\gamma(v)vf. \tag{20}$$

For the stationary situation (20) may be simplified by integration to

$$0 = T\frac{\partial f}{\partial v} + \gamma(v)vf, \tag{21}$$

which is solved by

$$f(v) = \mathcal{N}\exp\left[-\frac{V_{\mathrm{diss}}(v)}{T}\right]. \tag{22}$$

Inserting (18) we obtain

$$f(v) = \mathcal{N}\left(\kappa + v^2\right)^{\frac{\mu+\kappa}{2T}}\exp\left[-\frac{v^2}{2T}\right]. \tag{23}$$

The constant $\mathcal{N}$ has to be determined by normalization of $f(v)$. For the special case $\kappa = 0$ corresponding to particles without internal dissipation we get

$$\mathcal{N}^{-1} = (2T)^{\frac{T+\mu}{2T}}\,\Gamma\left(\frac{T+\mu}{2T}\right) \tag{24}$$

where the Euler Γ-function is defined by

$$\Gamma(z) = \int_0^\infty t^{z-1}\,\mathrm{e}^{-t}\,\mathrm{d}t. \tag{25}$$

In our model the single free particle situation is equivalent to a ring with $N = 1$. We tested the analytical result (23) by numerical simulations of the Langevin equations for a free particle with $F_i = 0$ and found a good agreement (see Fig. 3). As explained in the previous section, we can only expect a Maxwell-type probability density if the pumping is switched off.

The distribution function of an ideal $1d$-non-equilibrium gas with N non-interacting particles is simply given by

$$f(v_1, \ldots, v_N) = \Pi_{i=1}^N f(v_i). \tag{26}$$

For free particles the corresponding stationary FPE is obviously very easy to solve. Unfortunately this will be completely different if we include interactions between the particles. Hence if dealing with interacting particles we will return to the analysis of the Langevin equations (19) which represent an equivalent description of the stochastic dynamics (Fig. 3).

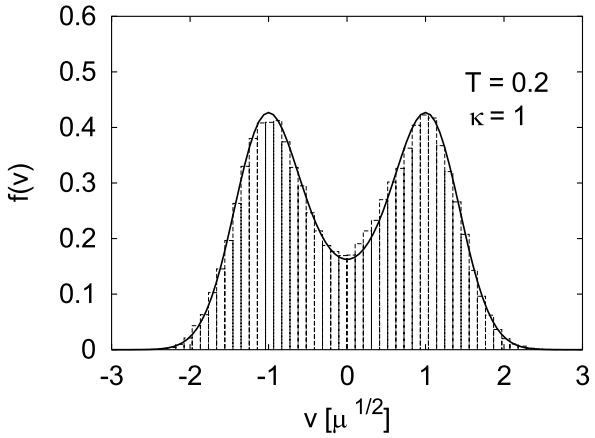

(a)

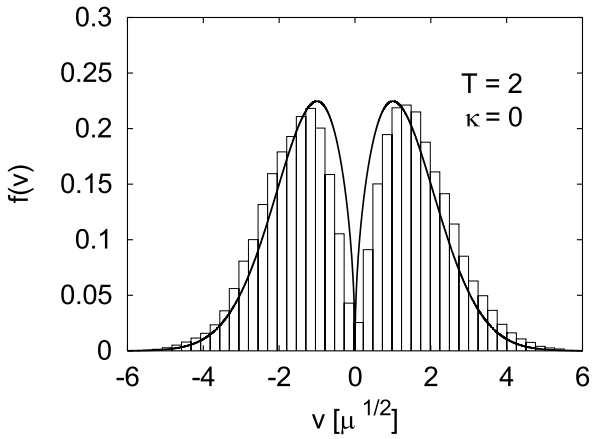

(b)

Fig. 3. The continuous line corresponds to the probability density analytically calculated from (23). The normalization constants were obtained by numerical integration. For the numerically calculated graphs (boxes) we generated histograms and divided by the box width.

3 Brownian particles with Morse interactions

3.1 Preliminary works

Before we start the discussion of Morse rings at non-zero temperature $T > 0$ we review relevant results from previous works. In [6] we analyzed Morse rings at $T = 0$. We found that depending on the density of particles $n = N/L$ there exist different particle configurations on the ring which minimize the potential energy U. Independent of the number N of particles the configuration with equal distances between all particles corresponds to a minimum as long as

$$n > \frac{b}{\ln 2 + b\sigma} = n_{\rm c}. \tag{27}$$

In the density region $n \gg n_{\rm c}$ Morse and Toda rings show qualitatively the same mono-stable behavior. For $n \to \infty$ Morse rings with parameter b behave like Toda rings with parameter $2b$. Moreover there exists a second critical value $\bar{n}_{\rm c}$ of the density such that for $n < \bar{n}_{\rm c}$ new minima of the potential energy appear. These are N equivalent configurations each corresponding to a single cluster of N particles. Between the two critical density values we have the relation $\bar{n}_{\rm c} \geq n_{\rm c}$ where $\bar{n}_{\rm c} = n_{\rm c}$ only if $N = 2$. We calculated $\bar{n}_{\rm c}$ for $N = 3$

$$\bar{n}_{\rm c}(3) = \frac{3b}{\ln \frac{27}{4} + 3b\sigma} > n_{\rm c} \tag{28}$$

and found that $\bar{n}_{\rm c}(N)$ increases monotonically with N but is bounded by $n = \sigma^{-1}$. These results mean that for $N \geq 3$ in the transition interval $(n_{\rm c}, \bar{n}_{\rm c})$ both the clusters and the uniform distribution represent local minima of the potential energy. For $n < n_{\rm c}$ only clusters correspond to stable configurations and we could evaluate $Z_N^s = 2^N - 2 - N$ for the number of saddle points (of arbitrary rank) in the $(N-1)$-dimensional potential energy landscape. These metastable points correspond to symmetric combinations of smaller clusters. In the pure cluster regime $n < n_{\rm c}$ the total number of equilibria is given by $Z_N = 2^N - 1$, *i.e.* we have N minima (cluster), Z_N^s saddles and 1 maximum (equal distances $1/n$ between the particles).

Having summarized the statics so far we will now give a short notice of the results obtained for the deterministic nonlinear dynamics at $T = 0$. For $\mu < 0$ corresponding to under-critical pumping the ring relaxes into one of the minima of the potential energy. In case of over-critical pumping we have to distinguish between the different density regimes. If $n > \bar{n}_{\rm c}$ the Morse ring is Toda-like and we may identify $N + 1$ qualitatively different attractors [5,11,15] representing stationary uniform rotations, 1-soliton solutions, 2-soliton solutions,... up to anti-phase oscillations in case of $N = even$. In fact the absolute number of attractors is bigger since there is for example index translation symmetry in the system. During the stationary uniform rotations the particles have occupied the minima of the potential energy. These types of attractors are always found independent from the density regime.

In the transition region $\bar{n}_{\rm c} > n > n_{\rm c}$ for weak over-critical pumping only the rotations and small stationary oscillations around the ground state configurations could be observed. By ground state configurations we mean a configuration of the particles that minimizes the full energy of the system. The same is true for $n_{\rm c} > n$ and weak pumping. Finally, for strong over-critical pumping we have again the Toda-like attractor structure in all density regimes since the exponentially repulsive forces of the potential dominate the dynamics. The expressions "strong" and "weak" pumping refer to $\mu \gg 2\Delta U_i$ and $\mu \ll 2\Delta U_i$ where ΔU_i is the depth of the minima of U. The two inequalities just reflect a comparison between kinetic and potential energy. In the intermediate $\bar{n}_{\rm c} > n > n_{\rm c}$ region there are two different values for ΔU_i (corresponding to the two types of minima) and both of them are relatively small. If $n_{\rm c} > n$ all ΔU_i take same values. For very low densities $n \to 0$ they may be approximated by the depth of the Morse potential $\Delta U^M = a/(2b)$.

Since the intermediate density region bears some more complications compared to the others we are rather going to concentrate on the low and high density limits. This is somewhat justified by the fact that the system responds to the special features of this region only at very weak internal pumping and very low temperatures.

3.2 Low temperature regime

At very low temperatures $0 < T \ll \mu$ the stochastic influence of the heat bath may be considered as a perturbation of the deterministic system with $T = 0$. Since the deterministic terms in the equations of motions (19) represent the dominating contributions to the dynamics of the system we may expect that the stationary behavior is still similar to the one described in the previous section. Thus a first approach to characterize the stochastic system described by Langevin equations (19) is trying to find out which attractors are favored by the Brownian particles at small $T > 0$. For the noisy system the word "attractor" must not be understood in the sense of its strict mathematical definition but it has to be seen as a useful description of such subsets of the phase space which are (on average) more frequently visited than others. At least at low temperatures these subsets are found near the original attractors of the deterministic system. Basically, we try to find out which types of active motions are more likely than others if noise is included.

For deterministic systems with $T = 0$ each attractor corresponds to a stable invariant subset $\mathcal{A}\epsilon\mathcal{P}$ of the phase space $\mathcal{P} = \{x_1, \ldots, x_N, v_1, \ldots, v_N\} = \{\boldsymbol{X}, \boldsymbol{V}\}$. Each trajectory $(\boldsymbol{X}(t), \boldsymbol{V}(t))$ may be characterized by the time averages

$$\langle Z\rangle_\tau = \frac{1}{\tau}\int_0^\tau Z(t)\,\mathrm{d}t \tag{29}$$

of physical quantities $Z(t) = Z(\boldsymbol{X}(t), \boldsymbol{V}(t))$ like kinetic energy, momenta etc. For $\tau \to \infty$ the system approaches the attractor $\mathcal{A}$ if the trajectory lies in the attractor basin $\mathcal{B}(\mathcal{A})\epsilon\mathcal{P}$ and we may define

$$\langle Z(\mathcal{A})\rangle = \lim_{\tau\to\infty}\langle Z\rangle_\tau. \tag{30}$$

If a system with a finite number of attractors is subject to stochastic initial conditions then the stationary probability density functions $f(\langle Z\rangle_\tau)$ at $T = 0$ are discrete and given by

$$f(\langle Z\rangle) = \sum_A p_\mathcal{A}\,\delta(\langle Z\rangle - \langle Z(\mathcal{A})\rangle). \tag{31}$$

The coefficients $p_\mathcal{A}$ are simply given by

$$p_\mathcal{A} = \frac{\mathrm{vol}[\mathcal{B}(\mathcal{A})]}{\mathrm{vol}[\mathcal{P}]} \tag{32}$$

where $\mathrm{vol}[\mathcal{B}(\mathcal{A})]$ is the phase space volume of the attractor basin $\mathcal{B}(\mathcal{A})$. The coefficients $p_\mathcal{A}$ may be determined experimentally by numerical simulations. We already used this method to identify the attractors of active Toda rings [5]. The procedure is straightforward in the way that one simply has to simulate the dynamical equations while at the same time measuring a certain quantity. Using the results $\langle Z\rangle$ of many runs with different initial conditions one generates histograms of the relative frequencies $h[\langle Z\rangle]$ and the density functions $f(\langle Z\rangle)$ may be obtained from the latter when dividing by the box width.

For our system the time average of the mean ensemble velocity $\langle Z\rangle = \langle\langle v\rangle_N\rangle \equiv \langle\langle v\rangle\rangle$ is defined by

$$\langle\langle v\rangle\rangle = \lim_{\tau\to\infty}\frac{1}{\tau}\int_0^\tau \frac{1}{N}\sum_{i=1}^N v_i(t)\,\mathrm{d}t. \tag{33}$$

This is a suitable quantity to describe stationary behavior *e.g.* for uniform rotations at $T = 0$ we would expect $\langle\langle v\rangle\rangle = \pm\sqrt{\mu}$. Additionally we are going to use the temporal average of the ensemble sum over mean square displacements $\langle Z\rangle = \langle\langle \Delta\rho^2\rangle_N\rangle$ from the average distance n^{-1} where

$$\langle \Delta\rho^2\rangle_N = \frac{1}{N(N-1)}\sum_{i=1}^N [\rho_i(t) - (1/n)]^2 \tag{34}$$

and $\rho_i = \sigma + r_i = 1 + r_i$. This quantity is minimal $\langle\langle \Delta\rho^2\rangle\rangle = 0$ for uniform rotations with equal distances between the particles and it increases for clustering states.

For $T > 0$ the approach explained above has to be slightly modified, the system may now switch between attractor regions due to the thermal fluctuations. Since we are interested in the most frequently visited phase space regions we rather measure time averages over many consecutive time intervals $\Delta\tau \gg 1$ of one single simulation run instead of calculating histograms over a large number of runs with different initial conditions as with $T = 0$.

In Figures 4–8 we plotted the results of our simulations for different parameter constellations. In all simulations we have fixed the parameter $\kappa = 1$ which just means that internal dissipation within the particles and conversion of depot energy into kinetic energy are equally large. The internal pumping is then controlled by μ. Because of the considerations in Section 3.1 we typically concentrate on the following two situations

1. Toda-like limit (mono-stable potential energy) characterized by $n \gg \bar{n}_\mathrm{c}$.
2. Low density limit $n < n_\mathrm{c}$ (multi-stable potential energy) and weak pumping $\mu \ll \Delta U$.

Only in the second case clusters may occur at low temperatures due to the multi-stability of the potential energy.

High density (Toda-like) Morse ring

We already mentioned above that for $T = 0$ we have $N+1$ qualitatively different attractors. Each of these attractors is characterized by different values of $\langle\langle v\rangle\rangle$ and $\langle\langle \Delta\rho^2\rangle\rangle$. In Figure 4 we plotted the histograms for the relative frequencies of appearance within 1000 runs with different initial conditions for a ring with $N = 4$. More exactly

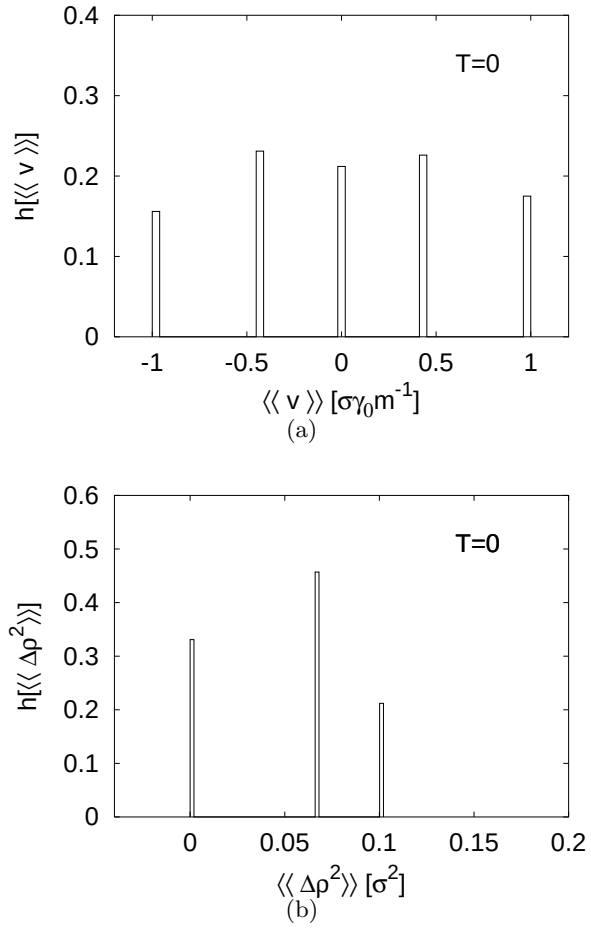

Fig. 4. Histograms for a high-density (Toda-like) Morse ring with $N = 4$ particles at $T = 0$, $n = 1.2 > \sigma^{-1}$, $\mu = 1$, $a = 1$, $b = 1$. The peaks at $\langle\langle v\rangle\rangle = \pm 1$ and $\langle\langle \Delta\rho^2\rangle\rangle = 0$ correspond to the rotation attractors, those at $\langle\langle v\rangle\rangle = 0$ and $\langle\langle \Delta\rho^2\rangle\rangle = 0.1$ to stationary, optical anti-phase oscillations of neighboring particles.

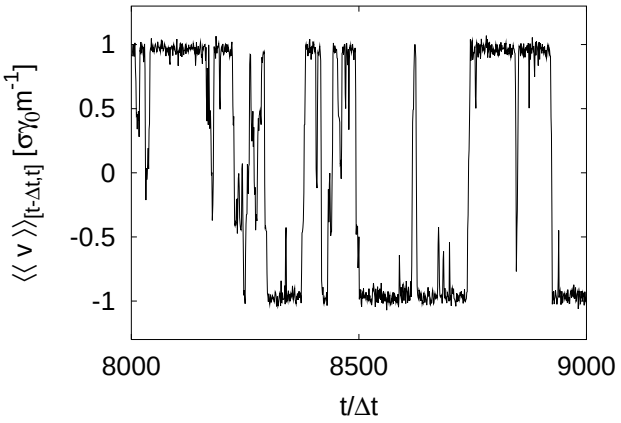

Fig. 5. Time averages $\langle\langle v\rangle\rangle$ for a Morse ring with $N = 4$ particles at $T = 0.05$, $n = 1.2$, $\mu = 1$, $a = 1$, $b = 1$. One can see that the regions close to the rotation attractors with $\langle\langle v\rangle\rangle = \pm 1$ are most frequently visited.

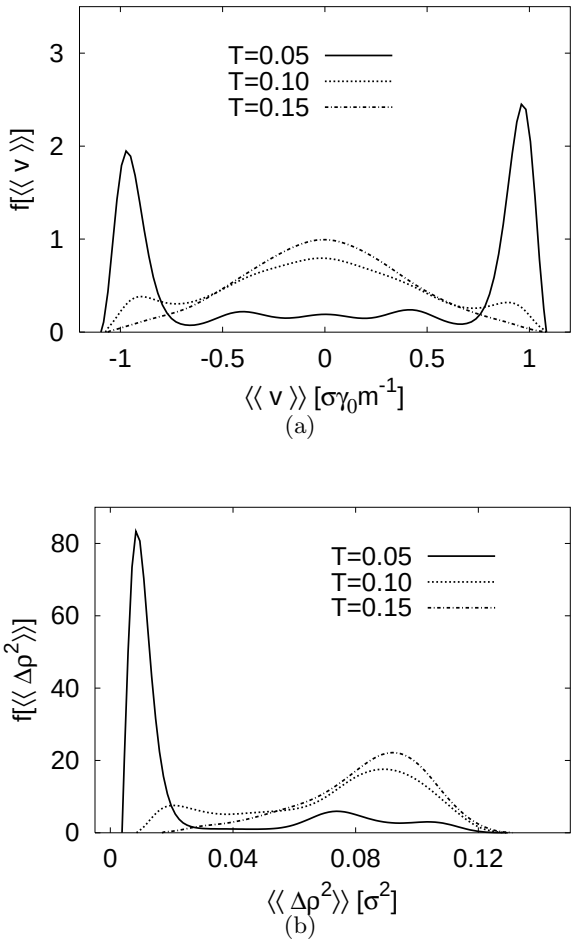

Fig. 6. Numerically generated probability densities for a (Toda-like) Morse ring with $N = 4$ Brownian particles, $n = 1.2$, $b = 1$, $a = 1$, $\mu = 1$ and $T > 0$. For illustrative reasons we have smoothened the numerically calculated curves in our pictures using bezier lines. At low temperatures the phase space regions near to the rotation attractors are more frequently visited than the others.

we always started with equal distances between all particles and initial velocities randomly taken from a standard normal distribution. If one had used random initial positions and momenta taken from uniform distributions the heights of the histogram boxes would give the experimental values of the $p_{\mathcal{A}}$ in (31). For all simulations we used the classical Euler algorithm with discretization intervals $\mathrm{d}t = 0.0001$ and the "stationary" time averages were measured between $25 < t < 50$.

In Figure 6 one can see how the probability density behaves when the temperature of the heat bath is increased. In agreement with the procedure described before we now used one long run and measured the time averages over 10^4 consecutive time intervals of length $\Delta t = 25$. The explicit results for $\langle\langle v\rangle\rangle$ taken over each of the 1000 measuring intervals between $t = 2\times 10^5$ and $t = 2.25\times 10^5$ are shown in Figure 5.

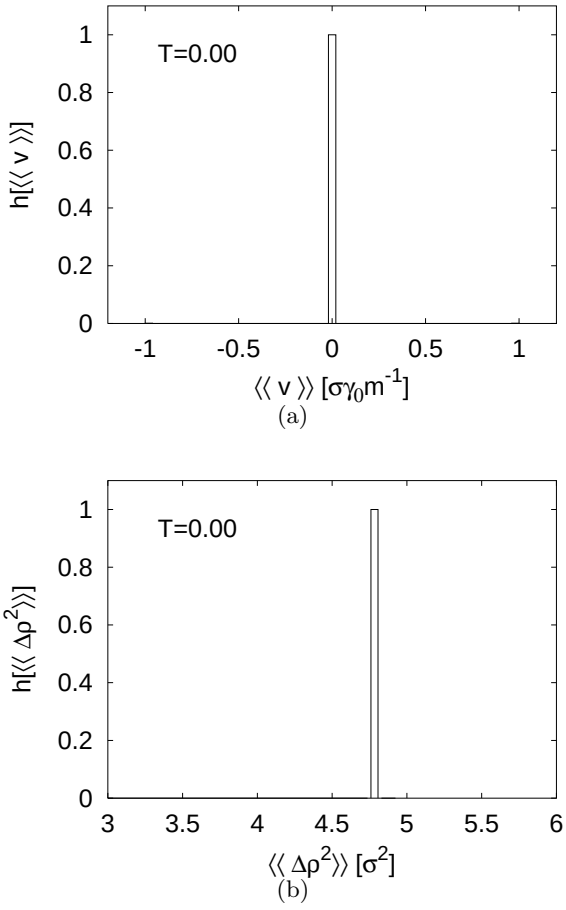

Fig. 7. Histograms for a low-density Morse ring with $N = 4$ particles at $T = 0$, $n = 0.3 < n_c = 0.59$, $\mu = 1$, $a = 10$, $b = 1$. Two very small peaks at $\langle\langle v\rangle\rangle = \pm 1$ corresponding to the rotation attractors are not visible since these attractors are very seldomly approached under the chosen stochastic initial conditions. Thus the visible peak corresponds to oscillations around the energy ground state *i.e.* anti-phase oscillations in clusters.

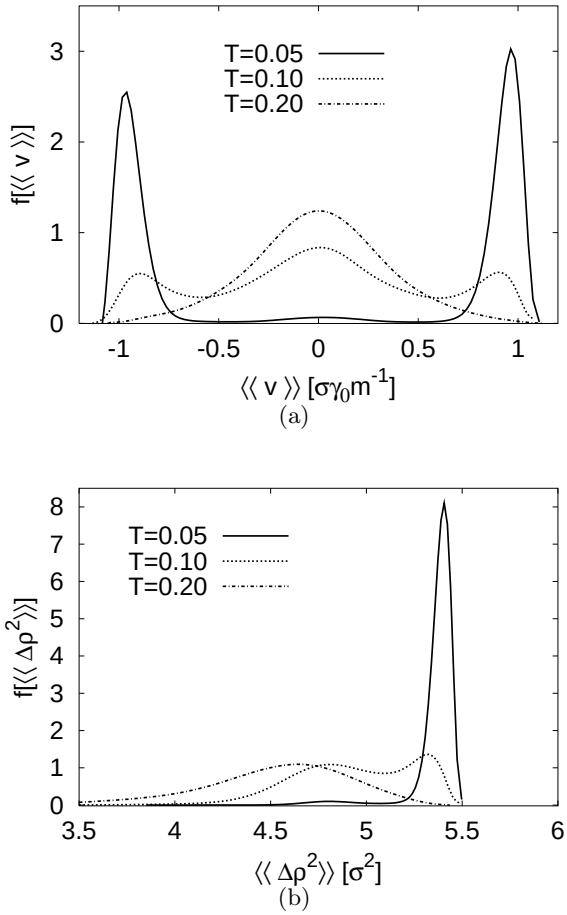

Fig. 8. Numerically generated probability densities for low-density Morse rings with $N = 4$, $n = 0.3$, $b = 1$, $a = 10$, $\mu = 1$ and $T > 0$. Again at low temperatures the phase space regions near to the rotation attractors are more frequently visited than the others. In the second diagram the peak at $\langle\langle \Delta\rho^2\rangle\rangle \approx 5.4$ (not visible in Fig. 7) for $T = 0.05$ gives the deviation for the cluster rotations.

From these simulations we calculated the probability densities. As is to be expected, for high temperatures the shape of the velocity densities comes close to a Gaussian since the stochastic forces dominate the dynamics in this region. The interesting effect can be observed at low temperatures. Here the system obviously prefers the rotation attractors in other words the more coherent motions.

Low density Morse ring

By choosing $n < n_c$ the potential energy U has N minima, each corresponding to a cluster configuration. The clusters my be distinguished by the index of the first particle of the cluster for example thus they only differ by index translations. For small pumping characterized by $0 < \mu/2 \ll \Delta U_i$ the deterministic system with $T = 0$ has only the rotation attractors (now cluster rotations) with $\langle\langle v\rangle\rangle = \pm\mu$ or secondly it may oscillate around the ground state indicated by $\langle\langle v\rangle\rangle = 0$. In Figure 7 we plotted the histograms for $T = 0$ corresponding to those from Figure 4. For stochastic initial conditions like before one can see that the attractor basins of the rotation attractors are only seldomly touched.

It is now interesting to see (Fig. 8) that for low temperatures the system is again more frequently driven close to the rotation attractors than to the other attractor regions. This seems to be a general property of this model and it should also be generalizable for similar systems. The argument leading to this conclusion is that at low temperatures the dynamics of the system is still closely connected to the potential energy $U(\boldsymbol{X})$. Due to the stochastic forces the systems may cross the separatrices dividing the phase space into attractor regions. According to numerical investigations the attractor basins of the incoherent motions are likely to be larger than those of the coherent motions but the coherent motions (rotations) minimize

$U(\boldsymbol{X})$ globally. Thus once the particles have taken such a minimizing configuration they need strong stochastic impacts from the heat bath to leave it. Consequently, for sufficiently low temperatures (*i.e.* weak fluctuations of the bath) it is more likely to observe rotation-like motions as compared to wavy motions. The critical temperature values T_c indicating the disappearance of the coherent motions in Figure 8 ($T_c \approx 0.12$ for $n = 1.2$, and $T_c \approx 0.13$ for $n = 0.3$) may also be seen as the natural limits for the concept of analysis pursued in this subsection. As soon as the stochastic influence of the heat bath on the dynamics becomes stronger than the deterministic pumping a thermodynamical approach seems to be more appropriate and effective. We shall proceed this way by treating the nonlinear pumping as a perturbation of the thermodynamical equilibrium system in the next section.

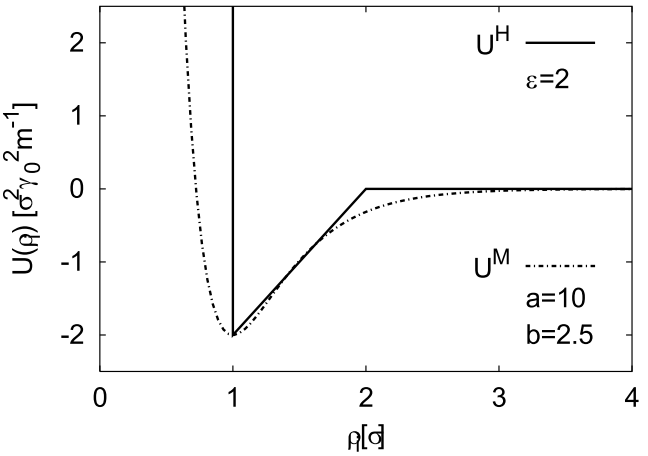

Fig. 9. All numerical results presented in this section refer to Morse potentials with parameters $a = 10$ and $b = 2.5$ giving a depth $\Delta U^M = 2$ of the potential.

3.3 Thermodynamical quantities

In this section we are interested in the behavior of typical thermodynamical quantities (*e.g.* pressure) in an active Morse ring with respect to variations of the essential parameters (temperature, pumping strength, density). Due to the previous considerations in Section 2.3 the physical temperature T of the heat bath is equal to the amplitude parameter of the stochastic forces D. The density n of the Morse ring is also self-evidently given (4) and the internal pumping of the particles is characterized by κ and μ. Thus the remaining quantity to be defined is the pressure P. A straightforward definition by the means of a partition function like in equilibrium statistical mechanics is not possible since we do not know the exact probability density for interacting, self-driven particles and, more importantly, there is no general rule at all for deriving the pressure from the partition functions of non-equilibrium systems. Thus in order to find a definition that is sensible from the physical point of view we have to try to adapt the strategy applied in kinetic theories. In ordinary $3d$-systems (*e.g.* gas in a box) P is given by the temporal average of the forces acting on a differential area of the boundaries (walls). Obviously there are two problems with our system: (1) It is $1d$ so there are no wall *areas* and (2) it has periodic boundary conditions, *i.e.* there is no real boundary at all. Looking for alternatives in our model it seems useful to consider P as the time average of the forces between neighboring particles *i.e.* we shall define P as internal pressure. Let us again think of the particles to be connected be springs. The energy of a single spring in the Morse ring is given by

$$U^M(\rho_i) = \frac{a}{2b}\left(\mathrm{e}^{-b(\rho_i-1)} - 1\right)^2 - \frac{a}{2b}\,. \tag{35}$$

Here we just rewrote the Morse potential from (1) using the actual distance coordinate $\rho_i = x_{i+1} - x_i$. Since we want P to be an intensive quantity it may be defined by

$$P = -\lim_{\tau\to\infty}\frac{1}{\tau}\int_0^\tau \frac{1}{N}\sum_{i=1}^{N}\frac{\mathrm{d}U^M(\rho_i)}{\mathrm{d}\rho_i}\,\mathrm{d}t. \tag{36}$$

It has to be interpreted as the average local compression or expansion of the ring and can be measured for both equilibrium and non-equilibrium systems. We can illustrate the above definition by considering the following configurations

1. For purely attracting forces the pressure is always negative.
2. For purely repulsive forces the pressure is always positive (*e.g.* in Morse rings with $L < 2$).

At $T = 0$ the ring possesses a certain static pressure. This static pressure is zero only if $n = 1/\sigma$ or $L = N\sigma$ respectively *i.e.* all springs are relaxed. In order to check analytically whether our definition (36) of the pressure is consistent with the definition given in equilibrium statistical mechanics we may look at the following simplification of the Morse interaction

$$U^H(\rho_i) = \begin{cases} \infty & \rho_i < \sigma \\ \frac{\varepsilon}{\sigma}(\rho_i - 2\sigma) & \sigma < \rho_i < 2\sigma \\ 0 & 2\sigma < \rho_i. \end{cases} \tag{37}$$

This potential models incompressible particles (*via* the hard-core part) of diameter σ with attractive short range interaction and is familiar to the *van-der-Waals* model [16]. A comparison of this potential with the Morse potentials is plotted in Figure 9 for the parameter setting used during the simulations. Compared to the Morse potential $U^H(\rho_i)$ has the advantage that at least for rings with $N = 2$ the statistical dynamics is analytically soluble. Thus we may use it to check the consistency of (36). Analytical discussions of the equilibrium thermodynamics of similar non-linearly interacting systems may be found in [17–19].

Using our unit system with $\sigma = 1$ the standard calculations [16,17] yield for the canonical sum over states of a ring with U^H and $N = 2$

$${Z_2}^I = \frac{\pi}{h^2\beta}(L-2)\,\mathrm{e}^{\beta(4-L)\varepsilon} \tag{38}$$

if the length is $2 < L < 3$,

$$Z_2{}^{II} = \frac{\pi}{h^2\beta}\left[\frac{2\mathrm{e}^{\beta\varepsilon}}{\beta\varepsilon} + \left(4 - L - \frac{2}{\beta\varepsilon}\right)\mathrm{e}^{\beta(4-L)\varepsilon}\right] \quad (39)$$

if $3 < L < 4$ and

$$Z_2{}^{III} = \frac{\pi}{h^2\beta}\left[\frac{2}{\beta\varepsilon}\left(\mathrm{e}^{\beta\varepsilon} - 1\right) + (L-4)\right] \quad (40)$$

if $4 < L$ where $\beta = 1/T$ (again $k = 1$) and h is Planck's constant. The free energy is given by

$$F = -\frac{1}{\beta}\,\ln Z_2 \quad (41)$$

and the pressure is its derivative with respect to the ring volume *i.e.* length

$$P = \left(-\frac{\partial F}{\partial L}\right)_T \quad (42)$$

at constant temperature. Thus we have explicitly

$$\begin{aligned} P^I &= -\varepsilon + \frac{T}{L-2} \\ P^{II} &= \frac{\pi}{h^2\beta^2}\frac{\mathrm{e}^{\beta(4-L)\varepsilon}}{Z_2^{II}}\left[1 + \beta\varepsilon(L-4)\right] \\ P^{III} &= \left[\frac{2}{\varepsilon}\left(\mathrm{e}^{\beta\varepsilon} - 1\right) + (L-4)\right]^{-1}. \end{aligned} \quad (43)$$

For the first transition length $L = 3$ the pressure is given by

$$P^I(3) = T - \varepsilon = P^{II}(3) \quad (44)$$

and for the second critical value $L = 4$ it reads

$$P^{II}(4) = \frac{\varepsilon}{2(\mathrm{e}^{\beta\varepsilon} - 1)} = P^{III}(4). \quad (45)$$

Additionally we have $P^I(2) \to \infty$ for $L \to 2$ and $T > 0$. In Figure 10 one can see the approximate agreement between the numerically calculated isotherms using definition (36) and the analytic curves based on (43). As to expect both diagrams show the typical structure known from the van-der-Waals model [16].

Having defined all essential quantities P, T, n, μ and κ consistently we are now able to generate the characteristic phase diagrams for the non-equilibrium systems with $\mu > -1$ by simply integrating the Langevin equations (19) numerically. We start again with smallest non-trivial ring with $N = 2$. In Figure 11 one can see the different pressure curves as functions of the density for different values of μ at a fixed temperature.

Obviously an increase of μ has an effect similar to an increase of T. Now it is also interesting to see what happens if we increase the number of particles. In Figure 12 we plotted the results for a ring containing $N = 10$ particles.

One can see that the density-temperature region featuring negative pressure is already significantly smaller compared to the case of $N = 2$. Again the additional energy take-up due to the pumping leads to deformations of the pressure curves similar to those obtained when the temperature is increased in the equilibrium system.

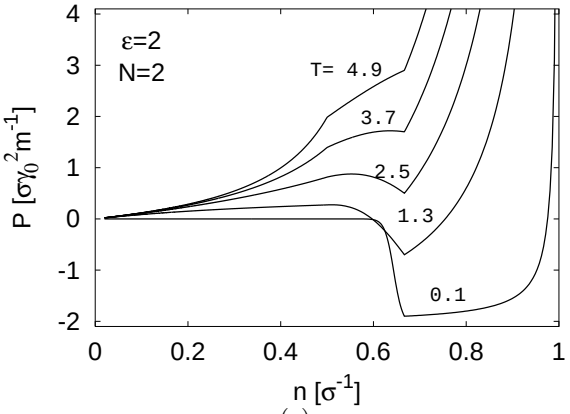

(a)

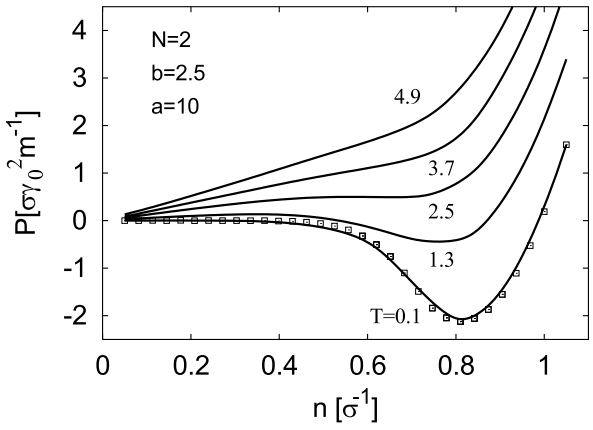

(b)

Fig. 10. Diagram (a) shows the analytically calculated curves for the potential U^H, and diagram (b) the numerically calculated equilibrium phase diagrams for the Morse ring. Throughout the remainder of the paper each curve calculated numerically from the Langevin equation is based on 30 equidistant points (with regard to the corresponding x-axis, here n-axis). For illustrative reasons we only plotted the measured points for the $T = 0.1$-isotherm in (b). In all subsequent diagrams we shall only represent the curves.

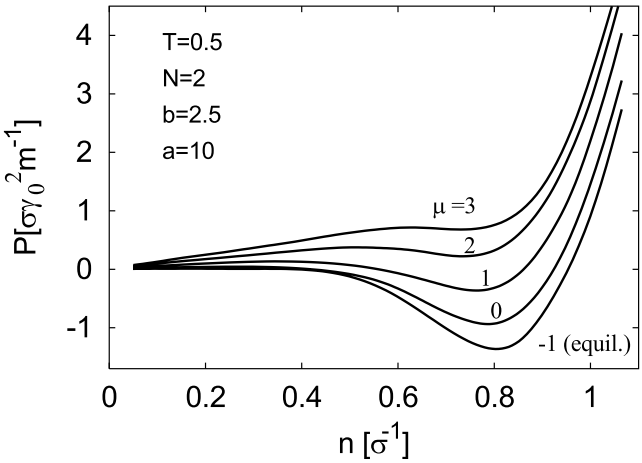

Fig. 11. Change in the phase diagram of the ($T = 0.5$)-isotherm for a Morse ring in presence of external pumping.

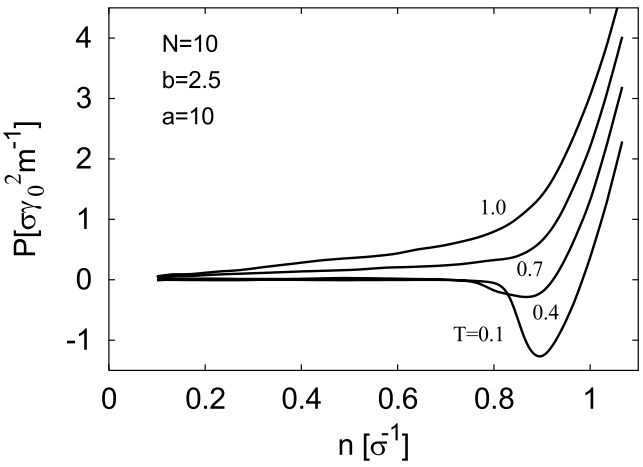

(a)

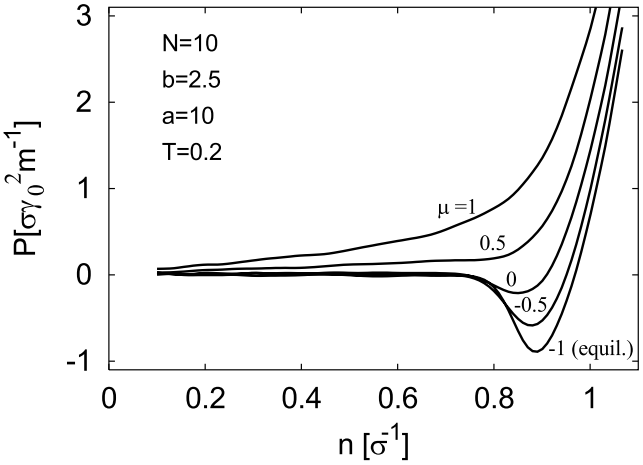

(b)

Fig. 12. The upper diagram shows isotherms of the equilibrium system and the lower diagram the change of the ($T=0.2$)-isotherm for different values of μ.

4 Transport in homogeneous external fields

Finally, we discuss the influence of a weak external homogeneous field K. We will assume that the Brownian particles are coupled to the field *via* a coupling constant e. Analogously to the procedure applied above we may choose a unit system such that $e = 1$, hence the full Langevin equation reads now

$$\frac{\mathrm{d}}{\mathrm{d}t}v_i - F_i = \left[\frac{1+\mu}{\kappa + v_i^2} - 1\right]v_i + K + A_i(t). \tag{46}$$

In the chosen unit system we have $[K] = \sigma\gamma_0^2 m^{-1} e^{-1}$. For $T = 0$ the external field breaks the right-left symmetry of the attractors which was also reflected in the histograms of Section 3.2. Since the orientation of the ring may be chosen arbitrarily so far it is sufficient to restrict the investigations on the case $K > 0$. This means that K itself defines an orientation for the ring. The natural quantity to characterize transport processes is the mean stationary current j which may be easily identified in our system with

$$j = e\,\langle\langle v\rangle\rangle = \langle\langle v\rangle\rangle. \tag{47}$$

The definition of $\langle\langle v\rangle\rangle$ was already given in (33)

$$\langle\langle v\rangle\rangle = \lim_{\tau\to\infty}\frac{1}{\tau}\int_0^\tau \frac{1}{N}\sum_{i=1}^N v_i(t)\,\mathrm{d}t.$$

and it allows us to measure j directly from computer experiments. If the stationary probability density for the velocities $f(v_1,\ldots,v_N)$ is known then j may as well be calculated analytically from

$$j = \frac{1}{N}\int\left[\Pi_{i=1}^N\,\mathrm{d}v_i\right] f(v_1,\ldots,v_N)\sum_{i=1}^N v_i. \tag{48}$$

Apparently the investigation of the current is only interesting in the presence of thermal fluctuations corresponding to $T > 0$. Due to the symmetry of the model we have $j = 0$ if the external field is switched off ($K = 0$).

4.1 Ideal non-equilibrium gas

The distribution function of the ideal $1d$-non-equilibrium gas (*i.e.* $F_i = 0$) with N particles is given by

$$f(v_1,\ldots,v_N) = \Pi_{i=1}^N f(v_i) \tag{49}$$

where $f(v_i)$ is the single particle distribution function of the ith particle (52). With respect to (48) the stationary current is given by

$$\begin{aligned} j &= \int\left[\Pi_{i=1}^N\,\mathrm{d}v_i\, f(v_i)\right]\left[\frac{1}{N}\sum_{i=1}^N v_i\right] \\ &= \int_{-\infty}^{\infty}\mathrm{d}v\; v\; f(v) \end{aligned} \tag{50}$$

where $f(v)$ is the probability of a single particle. Compared with (20) the probability density $f(v)$ is now determined by be the slightly modified FPE

$$\frac{\partial f}{\partial t} = T\frac{\partial^2 f}{\partial v^2} + \frac{\partial}{\partial v}\left\{\left[\gamma(v)v - K\right]f\right\}. \tag{51}$$

The stationary solution of (51) is

$$f(v) = \mathcal{N}'\exp\left[-\frac{V_{\mathrm{diss}}(v) - Kv}{T}\right]. \tag{52}$$

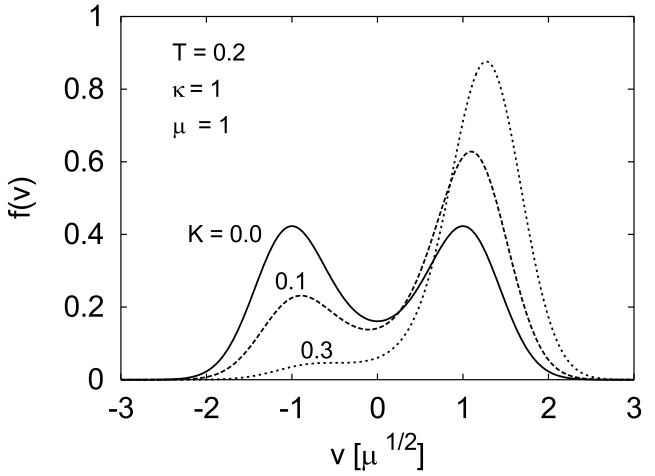

Fig. 13. The external field K breaks the symmetry of the stationary single particle probability density.

In Figure 13 the free single particle probability density $f(v)$ is shown for different values of the external field. For the special case $\kappa = 0$ corresponding to particles without internal dissipation we can solve (50) and find

$$j = K\left(1+\frac{\mu}{T}\right)\frac{{}_1\mathrm{F}_1\left[\frac{3T+\mu}{2T},\frac{3}{2},\frac{K^2}{2T}\right]}{{}_1\mathrm{F}_1\left[\frac{T+\mu}{2T},\frac{1}{2},\frac{K^2}{2T}\right]} \tag{53}$$

where the confluent hyper-geometric Kummer function is defined by

$$\begin{aligned}{}_1\mathrm{F}_1[a,b,z] &= 1+\frac{a}{b}\frac{z}{1!}+\frac{a(a+1)}{b(b+1)}\frac{z^2}{2!}+\ldots \\ &= \frac{\Gamma(b)}{\Gamma(b-a)\Gamma(a)}\int_0^1 \mathrm{e}^{zt}t^{a-1}(1-t)^{b-a-1}\,\mathrm{d}t.\end{aligned} \tag{54}$$

For weak fields $K \approx 0$ we may expand

$$j = K\left(1+\frac{\mu}{T}\right)\left(1-\frac{\mu}{3T^2}K^2\right)+\mathrm{O}(K^4). \tag{55}$$

Thus we observe a hyperbolical decrease of j for high temperatures. We may also use (55) to define a critical temperature T_c characterizing the transition from coherent motions to incoherent motions by demanding

$$\frac{\mathrm{d}}{\mathrm{d}T}\left[j-\mathrm{O}(K^4)\right]=0 \tag{56}$$

if $T = T_\mathrm{c}$. Then we obtain

$$T_\mathrm{c} = \frac{1}{3}\left(K^2+K\sqrt{K^2+9\mu}\right). \tag{57}$$

For $K \ll 3\sqrt{\mu}$ this may be simplified further

$$T_\mathrm{c} \approx K\sqrt{\mu}. \tag{58}$$

Using (58) in (55) the corresponding current is

$$j_\mathrm{c} = \frac{2}{3}(K+\sqrt{\mu}). \tag{59}$$

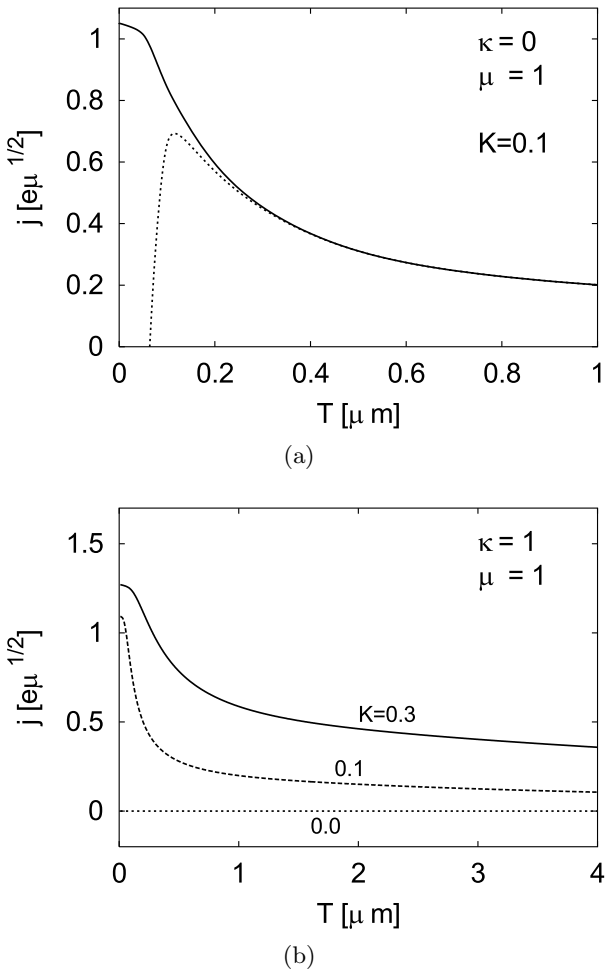

Fig. 14. (a) Analytically calculated current j (solid line) for a the ideal non-equilibrium gas with $\kappa = 0$ as a function of the temperature and approximation (dotted line) from (55). Parameters $K = 0.1$ and $\mu = 1$ give critical values $T_\mathrm{c} = 0.1$ and $j_\mathrm{c} = 0.73$. (b) Numerically integrated current for three different values of the external field and $\kappa > 0$. If the external field is switched off, $K = 0$, the probability density is symmetric and the mean current vanishes.

For $\kappa > 0$ the integral (50) has to be solved numerically and we plotted the results for $\kappa = 1$ and different values of K in Figure 14. As one can see in this picture the current decreases with increasing temperature. In the low temperature limit $T \to 0$ its maximum value is given by $j \approx \sqrt{\mu}+K$ corresponding to the global maximum of the single particle distribution function.

4.2 Interacting particles

For interacting particles we use again the Langevin approach and calculate the current with computer experiments *i.e.* we integrate (46) numerically and calculate the average current from the simulation data. With regard to the previous discussion in Section 3.1 we will restrict ourselves to the two most significant cases of mono-stable

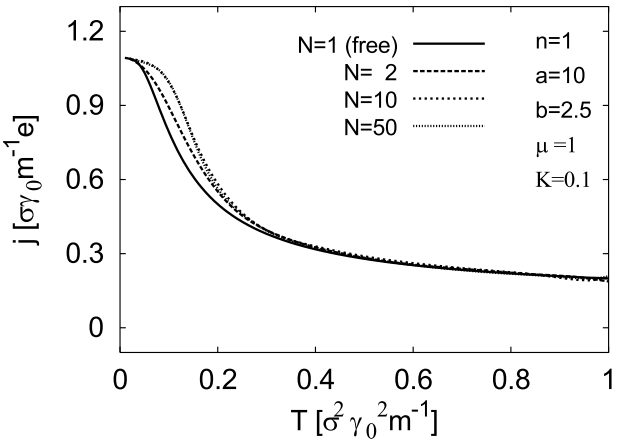

(a)

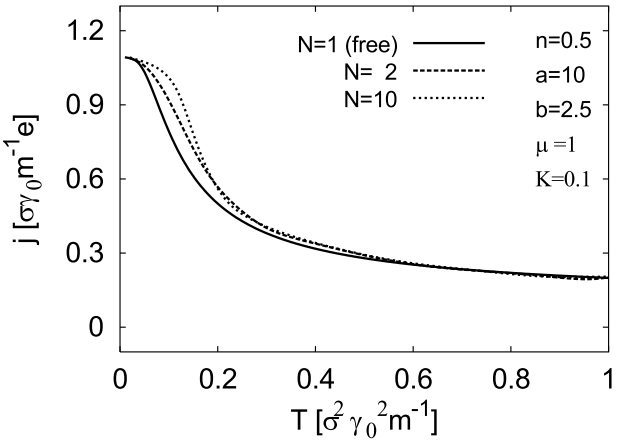

(b)

Fig. 15. Current in (a) Toda-like (high-density) Morse rings with $n = 1 > \bar{n}_c$ and (b) for low densities $n = 0.5 < n_c$. One can see that the shape of the curves is the same for both density regimes and qualitatively similar to those calculated for the free particle. For small N the region of enhanced mobility at low temperatures becomes slightly larger with increasing particle number. This effect is limited to small N as one can see from the diagram (a) where the curves for $N = 10$ and $N = 50$ coincide again.

(Toda-like) Morse rings with $n > \bar{n}_c$ and multi-stable Morse rings with $n < n_c$ and $\mu < \Delta U^M$. It is worth mentioning that only due to the non-linearity in the dissipative terms the interactions between the particles affect on the current in a ring. In Figure 15 one can see the results of our simulations for the rings with different density regimes and particle numbers. Obviously the numerical results obtained for interacting Brownian particles are very similar to the curves calculated for the free particle using the solution of the FPE (51). The results do not depend on the density of the rings. We may conclude that the type of interaction (attracting or repulsive) is only a minor factor for the transport behavior of the system. Nevertheless at small particle numbers the existence of a next-neighbor coupling leads to an increase of the critical temperature T_c characterizing the transition from high order ($j \approx \sqrt{\mu}+K$) at low temperatures $T < T_c$ to low order ($j \approx K$) for $T > T_c$. For the diagrams in Figure 15 we may estimate $0.1 \leq T_c \leq 0.2$. The results found in presence of the external field are in agreement with those from the symmetric situation $K = 0$ in Section 3.2 where we also observed a dominance of coherent motions at small temperatures.

5 Conclusion

In this work we discussed an $1d$-model of active Brownian particles with periodic boundary conditions. We considered Morse-interaction between neighboring particles which are repulsive at short distances and attracting at intermediate distances. Using this type of interaction our model converges to the well-known Toda model at large densities, while at low densities cluster may arise. The coupling to a heat bath was modeled by Gaussian white noise and additionally the particles were provided with internal energy depots. Due to conversion of depot energy into kinetic energy the particles possess the property to move actively.

In Section 2.3 we postulated that the Einstein relation is the correct fluctuation-dissipation-theorem for this model although there is a nonlinear effective friction term in the Langevin equations for the system. For the non-equilibrium system this lead to a probability density $f(v_1, \ldots, v_N)$ essentially differing from those of Maxwell-type equilibrium distributions.

Because of the two competing influences on the dynamics (deterministic nonlinear pumping and stochastic forces) we chose two different approaches to characterize our model. We started from the low temperature regime where the deterministic pumping dominates the dynamics. On the basis of extensive computer simulations we found that for low temperatures the system visits the coherent motions (*e.g.* cluster rotations) more frequently. We suppose that this is due to the fact that during the coherent motions the potential energy of the system is minimized. This effect should be generalizable to related classes of models and also utilizable in applications.

For high temperatures a thermodynamical description of the system turned out to be more convenient. In Section 3.3 we introduced the pressure for our model and investigated the non-equilibrium phase-diagrams. Effectively, the additional energy conversion from the depots has similar effects like an increase of the temperature in the corresponding equilibrium system. The structure of the phase diagrams is the same as in the diagrams of the well-known van-der-Waals model. Because of the periodic boundary conditions and the properties of the Morse interactions there also exists a temperature-density regime featuring negative pressure (*i.e.* if it could the ring would shrink). The size of the region where this effect exists decreases with increasing particle number.

The last part of the paper we dedicated to transport phenomena which may be observed in presence of external

fields. The combination of active motion and external field leads to enhanced mobility at low temperatures.

In conclusion we may say that although it is only a $1d$-model the investigated system shows a number of interesting effects which reflect some of the phenomena found in more complex systems. If we keep in mind the motivation of the pumping term [4] it is certainly difficult to apply this model to "purely" physical systems but we already indicated a possible interpretation of the model with respect to biological systems. In principle the model bears strongly simplified three basic features of real ecological systems

- interactions between neighbors including repulsion and attraction;
- energy take up (like *e.g.* food, petrol) and conversion into active motion;
- stochastic interactions with an environment.

In this sense also the originally purely physical quantities "pressure", "current" and "temperature" can be translated into more general context. For example one could consider the pressure in our model as the quantity measuring the tendency of system either to expand or to become compressed. Analogously the current is a simple measure for collective motion and the temperature a parameter for the noise generated by the environment. From that point of view we hope that our work contributes to the development of toy models for more complex processes in nature.

The authors are very grateful to M. Jenssen, P.S. Landa, L. Schimansky-Geier and V. Ushakov for valuable discussions. This work was supported by the DFG *via* the SfB555 (J.D. and U.E.) and by the Humboldt-Mutis Foundation (W.E.).

References

1. A. Einstein, M. von Smoluchowski. *Untersuchungen über die Theorie der Brownschen Bewegung/Abhandlungen über die Brownsche Bewegung und verwandte Erscheinungen*, Vol. 199, 3d edn. (Harri Deutsch, Frankfurt, 1999).
2. M. Schienbein, H. Gruler, Bull. Math. Biology **55**, 585 (1993).
3. A.S. Mikhailov, D. Zanette, Phys. Rev. E **60**, 4571 (1999).
4. W. Ebeling, F. Schweitzer, B. Tilch, BioSystems **49**, 17 (1999).
5. W. Ebeling, U. Erdmann, J. Dunkel, M. Jenssen, J. Stat. Phys. **101**, 443 (2000).
6. J. Dunkel, W. Ebeling, U. Erdmann, V.A. Makarov, Int. J. Bif. Chaos, in press, 2001.
7. M. Toda, *Nonlinear Waves and Solitons.* Kluwer Acad. Publ., Dordrecht, 1983.
8. M. Toda, N. Saitoh, J. Phys. Soc. Jpn **52**, 3703 (1983).
9. W. Ebeling, M. Jenssen, Y.M. Romanowsky, in *Irreversible Processes and Selforganization* (Teubner, Leipzig, 1989).
10. V. Makarov, W. Ebeling, M. Velarde, Int. J. Bifurc. Chaos **10**, 1075 (2000).
11. W. Ebeling, P.S. Landa, V. Ushakov, Phys. Rev. E **63**, 046601 (2001).
12. F. Schweitzer, W. Ebeling, B. Tilch, Phys. Rev. Lett. **80**, 5044 (1998).
13. U. Erdmann, W. Ebeling, L. Schimansky-Geier, F. Schweitzer, Eur. Phys. J. B **15**, 105 (2000).
14. Yu.L. Klimontovich, Physics-Uspekhi **37**, 737 (1994).
15. V.A. Makarov, E. del Rio, W. Ebeling, M.G. Velarde, Phys. Rev. E **64**, 036601 (2001).
16. F. Schwabl, Statistische Mechanik (Springer, 2000).
17. R.P. Feynman, *Statistical Mechanics* (Benjamin, Mass., 1972).
18. J.K. Percus, *Studies Statist. Mech.* **13**, 1 (1987).
19. M. Kac, G.E. Uhlenbeck, P.C. Hemmer, J. Math. Phys. **4**, 216 (1963).